LED-pumped passively Q-switched Cr:LiSAF laser

P. Pichon, Frédéric Druon, Jean-Philippe Blanchot, François Balembois, Patrick Georges

LED-pumped passively Q-switched Cr:LiSAF laser

Patrick Georges, P. Pichon, Frédéric Druon, Jean-Philippe Blanchot, François Balembois

LED-pumped passively Q-switched Cr:LiSAF laser

PIERRE PICHON,[1,2,*] FREDERIC DRUON,[1] JEAN-PHILIPPE BLANCHOT,[2] FRANÇOIS BALEMBOIS[1] AND PATRICK GEORGES[1]

[1]*Laboratoire Charles Fabry, Institut d'Optique Graduate School CNRS, Université Paris-Saclay, 91127, Palaiseau Cedex, France*
[2]*Effilux, 1 rue de Terre Neuve, 91940, les Ulis, France*
**Corresponding author: pierre.pichon@institutoptique.fr*

Received XX Month XXXX; revised XX Month, XXXX; accepted XX Month XXXX; posted XX Month XXXX (Doc. ID XXXXX); published XX Month XXXX

We report the first light-emitting diode (LED)-pumped Cr:LiSAF laser both in quasi-continuous-wave (qcw) and passively Q-switched operation. This work is based on the recent development of LED-pumped luminescent concentrators. Combining the capacity of high density integration of blue LEDs with the excellent properties of Ce:YAG luminescent concentrators, this new pump source can deliver high irradiance (7.3 kW/cm²) in the visible to pump Cr:LiSAF. The Cr:LiSAF laser demonstrates an energy of 8.4 mJ at 850 nm in qcw (250 µs-pulses at 10 Hz). A small-signal-gain per roundtrip of 1.44 at 850 nm and a wavelength tunability between 810 nm and 960 nm have been performed. A passively-Q-switched oscillator is also presented using a Cr:YAG saturable absorber. A peak power of 3.1 kW is obtained with pulse energy of 130 µJ and duration of 41.6 ns.

OCIS codes: *(230.3670) Light-emitting diodes; (220.1770) Concentrators; (140.5560) Pumping; (140.3580) Lasers, solid-state; (140.3540) Lasers, Q-switched; (140.3600) Lasers, tunable.*

http://dx.doi.org/10.1364/OL.99.099999

Transition metal-doped gain media (such as Ti:Sapphire, Cr:LiSAF, Alexandrite, etc.) are very attractive for near infrared broadband tunable lasers which can address a wide range of applications like remote sensing, medicine or material processing. Unfortunately, these materials absorb in the visible (from green to red), a spectral range where the pump sources are not optimal. Frequency doubled Nd-doped lasers at 532 nm and 671 nm are costly and complex and visible laser diodes are not as efficient as their infrared counterparts. This strongly limits the applicative and industrial impact of transition metal doped lasers. It appears then promising to explore alternative visible pumping based on the impressive development of visible light-emitting diodes (LEDs). Up to very recently, LED-pumping was limited to high gain media able to operate at low pump irradiance (like Nd^{3+} doped crystals [1-4]). Indeed, the LED irradiance in continuous wave regime is limited to 100 W/cm² whereas transition metal lasers require pump irradiance in the kW/cm² range to reach the oscillation threshold.

We have recently demonstrated that LED pumped luminescent concentrators (LC) are among the incoherent light sources with the greatest irradiance (several kW/cm² in pulsed regime [5]). Indeed, luminescent concentrators have the property to circumvent the brightness conservation rule with a process of absorption/emission in a high refractive index medium at the cost of a wavelength shift. Moreover, unlike direct LED pumping, LCs offer the potential of power scaling thank to the conversion of massive collection of LED beams into a small emitting area. Despite a cost in efficiency, this new kind of source benefits from all the advantages of the LED technology such as ruggedness, compactness, simplicity and low price [5-7]. For validation, LCs were used to pump rare-earth-doped crystals (Nd:YVO_4 [5] and Nd:YAG [8]). Recently, we have demonstrated the first LED-pumped alexandrite laser with a LC [9]: this opens the route to the pumping of other transition doped materials. The main advantages of LEDs compared to laser diodes are the robustness and the low cost but they cannot compete with their good beam quality (possibility to overlap the pump mode and laser mode) and peak brightness as an LED-pumped LC emits around $3x10^3$ W/cm²/sr when red laser diode will emit around $2x10^6$ W/cm²/sr. Compared to flashlamps which are limited to repetition rates of tens of Hz, LEDs have a longer lifetime, a better stability and ruggedness and they can access to higher repetition rates up to the cw regime.

In the late 80's, synthetic materials based on several declinations of Cr^{3+}-doped colquiriites (Cr:LiCAF, Cr:LiSAF and Cr:LiSGaF) were developed in order to challenge Ti:Sapphire (Ti:Sa) large gain bandwidth [10]. Indeed, Cr:LiSAF has remarkable performances in term of tunability (from 770 nm to 1110 nm [11]) and Cr^{3+} lifetime reaches 67 µs at 300 K (compared to 3.2 µs for Ti:Sa) which enable to store much more energy. After the first Cr:LiSAF laser performance in 1989 [10], pumped with a Kr gas laser, several solid-state lasers were anecdotally used as pump sources such as an alexandrite laser [12] or a ruby laser [13] and more recently with the frequency doubling of the 1.34 µm line of Nd:YVO_4 [14]. Cr:LiSAF was traditionally pumped by flashlamps [15-16] and red laser diodes [11, 17-19] mainly for tunable pulsed oscillators [18], amplifiers [19] and femtosecond lasers [17].

In this paper we investigate for the first time LED pumping of Cr:LiSAF with a luminescent concentrator. We explore laser performance in pulsed oscillators including different

measurements: gain, tunability, energy and pulse duration. We also investigated passive Q-switching of Cr:LiSAF with a Cr:YAG saturable absorber in the perspective to develop compact low cost laser sources tunable in the near infrared.

The luminescent concentrator used in this work is a 1 x 14 x 200 mm^3 Ce:YAG slab (composed of two 100 mm-long slabs bonded together with a UV-curing optical adhesive). A total of 2240 blue LEDs are placed close to both large facets (14 x 200 mm^2). Considering the 1 mm^2 emitting surface of each LED chip, this corresponds to a filling factor of 41 %. The blue light at 450 nm from the LEDs is absorbed by the Ce^{3+} ions and reemitted in the yellow-orange (centered at 550 nm, see Fig. 1). Because this emission occurs into the LC (refractive index of Ce:YAG is 1.82), a significant part of the emitted light is guided via total internal reflections up to the two small facets (1mm x14 mm) of the slab. The first facet is directly bonded to the gain medium in a transverse pumping configuration (Fig. 2) with an index matching UV-curing optical adhesive. The light emitted by the second small facet is reflected back to the LC by a plane mirror put very close to the LC. All the other facets have been let free in order to avoid any frustration of total internal reflections. Several losses occur in the luminescent concentration process. In our case the most significant losses are due to the Fresnel losses at the air/Ce:YAG interface (losses of 11%), the trapping and extraction efficiencies and the quantum shift. A part of the light from the LEDs is not absorbed and a part of the emitted light is reabsorbed but in a limited proportion with Ce:YAG (see [7]).

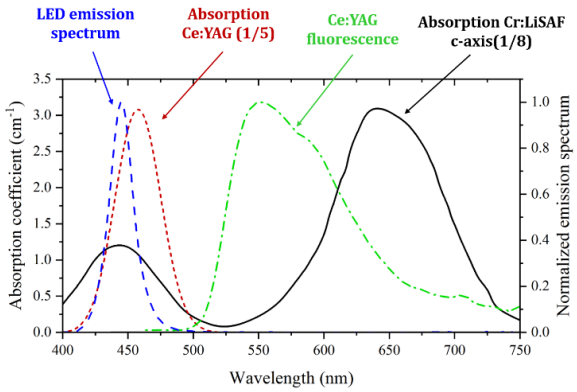

Fig. 1. Emission and absorption spectra: (blue) LED emission, (red) Ce :YAG absorption, (green) Ce :YAG emission, (black) Cr:LiSAF absorption for polarization parallel to the c-axis. The graph only indicates absorption for polarization parallel to the c-axis. Pump light being unpolarized, it has to be mentioned that for polarization parallel to the a-axis, the absorption coefficient is almost halved reaching 12.2 cm^{-1} at 650 nm.

LEDs (LUXEON Z from Lumileds) are driven in a pulsed regime at 10 Hz with pulse duration of 250 µs (4 times Cr^{3+} lifetime at 300 K in LiSAF) for a maximal current of 5 A chosen to operate the LEDs safely. In pulsed regime, the maximum peak irradiance of the LED is increased to 315 W/cm^2 (whereas it is set to 90 W/cm^2 in continuous wave regime). This results in an emission of 0.79 mJ per LED and a total energy of 1.76 J delivered by the 2240 LEDs to the LC. The energy delivered in the Cr:LiSAF reaches 257 mJ corresponding to a conversion efficiency of 14.6 % (see [5]). Despite this modest conversion efficiency value, the irradiance is increased by 23: from 315 W/cm^2 for one LED to 7.3 kW/cm^2 at the concentrator's output facet. The portion of the pump absorbed by the gain media is 43.5 % mainly due to the part of the pump light which does not stand under the absorption spectrum of Cr:LiSAF.
A 2.5 x 1 x 14 mm^3 Cr:LiSAF crystal with 5.5 at.% concentration is used. The laser facets of the crystals are cut at the Brewster angle and the axis orientation has been chosen to maximize the absorption of the pump light (polarization parallel to the c-axis, see Fig. 2).

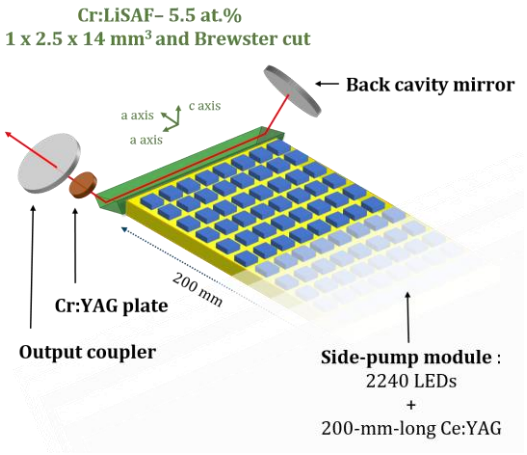

Fig. 2. Setup of the experiments. The back-cavity mirror has a 300 mm radius of curvature and is highly reflective between 610 nm and 1040 nm. Several output couplers are used with transmissions between 1% and 20% in the 650 nm-1000 nm range. A small part at the edges of the crystal is not pumped due to the Brewster geometry. For free-running operation, the cavity is 95-mm-long. The insertion of a SF10 prism for wavelength tunability results in a longer cavity (190-mm-long). For the small signal gain measurement process, calibrated losses are added with a N-BK7 window (leading to a 160-mm-long cavity). For passive Q-switched operation, a Cr:YAG plate is inserted resulting in a 110-mm-long oscillator.

First, a plano-concave cavity is performed with a high reflective back cavity mirror (radius of curvature of 300 mm) and a plane output coupler with transmissions of 2% (Fig. 2). The laser energy versus pump energy is plotted on Fig. 3a). A maximum energy of 8.4 mJ is measured for a pump energy of 227 mJ delivered to the gain medium by the luminescent concentrator. This corresponds to a concentrator/laser optical conversion efficiency of 3.7 % and an LED/laser optical conversion efficiency of 0.54 %. The maximum of energy is obtained when the laser operates in a $TEM_{11.0}$ mode (Fig. 3a inset) at 848 nm (Fig. 3b): this strong ellipticity could be explained by the crystal geometry (1mm x 2.5 mm) coupled with an absorption length typically in the order of a few mm for the yellow pump light. We adjust the cavity mirrors to operate in the TEM_{00} mode and 3.1 mJ has been demonstrated for a pump power of 227 mJ. A roll-off in the efficiency is clearly observed and will be discussed in the following with small signal gain measurements.

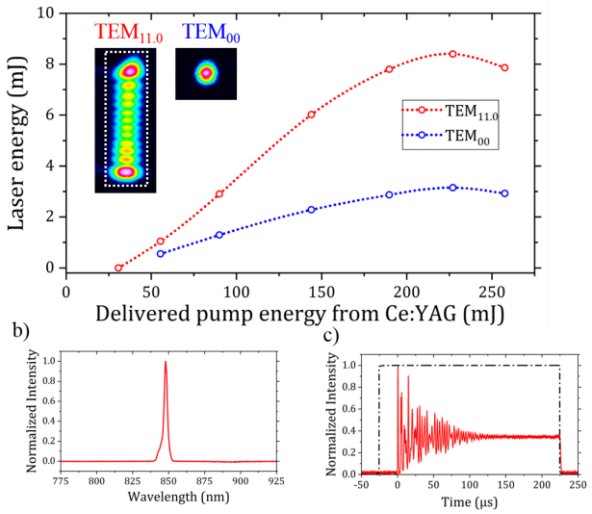

Fig. 3. a) Laser output energy versus pumping energy for a 2.0 % transmissions output coupler for $TEM_{11.0}$ (red) and TEM_{00} (blue) spatial modes. Inset: $TEM_{11.0}$ and TEM_{00} spatial profile of the laser. b) Laser spectrum in free running operation ($TEM_{11.0}$). c) Laser temporal profile for $TEM_{11.0}$ operation overlaid with LEDs time activation (black dashed and dotted line). The temporal profile corresponds to a pump energy of 150 mJ, before the decrease of power due to thermal effects.

We then investigate the spectral tunability of the laser. The cavity is extended (from 95 mm to 190 mm) in order to insert a SF10 prism. A continuous tunability from 810 nm to 960 nm is performed, the laser energy is reported in Fig. 4 as a function of the laser wavelength with a 2% output coupler. Lower energies have been obtained with this extended cavity compared to the 95-mm-long cavity because the laser beam in the Cr:LiSAF crystal is smaller than the $TEM_{11.0}$ mode previously measured leading to a reduced overlap with the gain volume in the crystal.

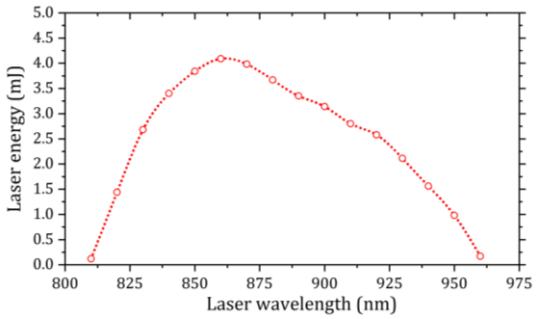

Fig. 4. Laser energy as a function of the laser wavelength. The cavity length is 190 mm.

The small-signal-gain is measured monitoring the laser threshold versus calibrated intracavity losses [20]. Calibrated losses are controlled by turning an 8 mm thick NBK-7 window. The small signal gain versus the pump energy is plotted on Fig. 5. For all points, we observe that the laser emission remains at 850 nm, in agreement with the maximum emission cross section of Cr:LiSAF. A maximum small-signal-gain of 1.44 per round-trip is measured. This experiment gives also a measurement of the intracavity losses (Findlay-Clay method [21]): the cavity presents passive losses per roundtrip of 1.3 %. A roll-off in the efficiency is clearly observed when increasing the pump power. This effect of roll-off in the Cr:LiSAF crystal is well known [18] and mainly due to thermal quenching and Auger upconversion. This comes from an increase of non-radiative decay that tends to increase further the temperature. In order to characterize this phenomenon, the fluorescence lifetime of Cr^{3+} ions has been measured as a function of the pump power. It decreases from 60.0 µs at low pump energy down to 26.9 µs at maximum pump energy (Fig. 5).

The double-pass small-signal-gain is numerically simulated. Simulations includes the main characteristics of Cr:LiSAF such as emission and absorption cross sections, passive losses and thermal quenching (using the lifetime measurements) . The pump density is estimated with a Monte Carlo ray tracing simulation (LightTools®) including spectral data: emission spectrum of Ce:YAG and absorption cross sections of Cr:LiSAF. Given the Lambertian emission of LEDs, in this ray-tracing simulation, the 2240 LEDs are approximated by two emitting surfaces delivering an equivalent power and situated above and underneath the luminescent concentrator. The pump density is estimated averaging the data collected on a plane detector at the center of the gain medium (inset Fig. 5). The simulations correctly corroborate the experimental data and the effect of temperature quenching clearly emerges.

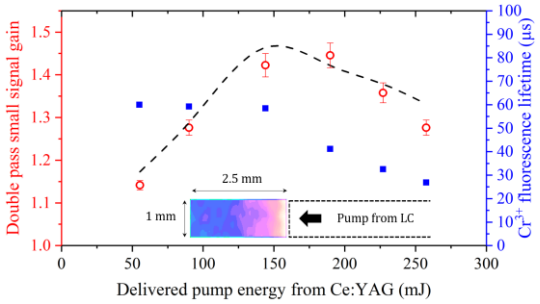

Fig. 5. Measurements (red circles) and simulation (dashed line) of the small signal gain per double pass and Cr^{3+} fluorescence lifetime (measured with a photodiode, blue squares) versus the pump energy. Inset : example of spatial repartition of the pump density ranging from 4 kW/cm^2 (blue) to 7.3 kW/cm^2 (white).

Knowing the gain, we can design a cavity to perform passive Q-switching with appropriate saturable losses. Passive Q-switching has indeed already been demonstrated for Cr:LiSAF with Cr:YSO [22] and for Cr:LiCAF with V:YAG [23]. In this experiment, we chose to investigate Cr:YAG since it is much more widespread through its use at 1064 nm and for its large absorption band matching the Cr:LiSAF emission. The Cr:YAG sample is 1.5-mm thick with a transmission T_0=89 % at 850 nm (corresponding to a Cr^{4+} concentration of 4.7 x 10^{17} cm^{-3}). The cavity length is 110 mm. Passively Q-switched regime has then been obtained for TEM_{00} laser mode. In this part of the study, the Cr:LiSAF crystal is cooled as it is directly in contact with a water cooled heat sink. The pulse energy and duration versus the output coupler transmission are reported in Fig. 6. In order to obtain a single pulse per pump cycle, the pump duration is adjusted close to the pulse buildup time

(indicated on Fig. 6). The pump energy varies from 30 mJ for the 2.0% output coupler to 60 mJ for the 20% output coupler. The pulse durations versus the output coupler transmission slightly vary around 40 ns to 50 ns. The highest peak power reached is 3.1 kW for a 41.6 ns pulse and 130 µJ energy with the 14% transmission output coupler (Fig. 7). This laser source is hardly comparable with other systems as very few flashlamp pumped and none laser diode pump passively Q-switched Cr:LiSAF lasers have been reported. Nevertheless, the system presented in this paper has similar pulse durations than works reported previously in passive Q-Switched operation [22, 23]. If the energy per pulse is lower than previous achievements, the Q-switched source presented in this work has the advantage of being single pulse, single transverse (TEM_{00}) and pumped by LEDs.

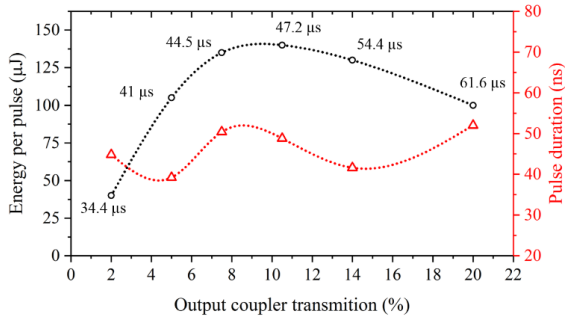

Fig. 6. Energy and pulse duration in Q-switched operation as a function of the output coupler transmission, for a T_0 = 89% transmission Cr:YAG saturable absorber at 850 nm and a TEM_{00}. Build-up time is indicated on the energy curves. The cavity length is 110 mm.

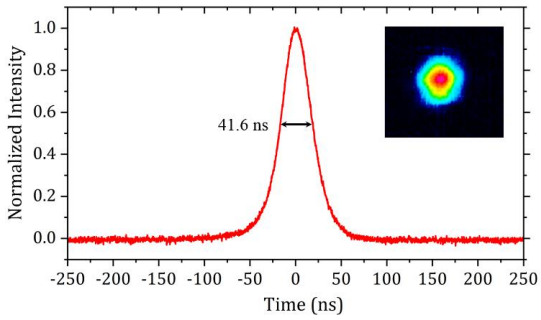

Fig. 7. Temporal and spatial profiles of the laser pulse emitted in passively Q-switched regime for the highest peak power (41.6 ns and 130 µJ) obtained with an output coupler transmission of 14 %.

To conclude, the first LED-pumped Cr:LiSAF laser has been characterized in qcw free-running operation at 10 Hz for 250 µs pump pulses leading to output powers up to 8.4 mJ and a tunability between 810 nm and 960 nm. This paper presents, to the best of our knowledge, the first passively Q-Switched Cr:LiSAF laser with a Cr:YAG saturable absorber (3.1 kW for 130 µJ and 41.6 ns pulses). The key benefit of this last performance lies in the technological maturity and availability of Cr:YAG crystals combined with the properties of LED pumping.

Several improvements can be performed such as an optimization of the pulsewidth in the qcw regime and an operation at higher repetition rate. There is no fundamental limitation for the repetition rate. In our case, we are limited by two technological issues: the pumping head cooling system and the power supply of the LEDs designed to nominally operate at 10 Hz. For the pump energy scaling, one way would be to use a longer gain medium together with the other unused facets. Another improvement of the system would be to improve the spectral matching between the LC and the gain medium by using for example Cr:LiCAF.

The laser presented in this paper is the first brick of targeted low-cost nanosecond sources in the UV after second or third harmonic generation. In addition, we reported the highest small signal gain ever obtained for an LED-pumped transition-metal-doped laser: 1.44. This confirms the interest of LED-pumping for tangible applications: LED-pumped Cr:LiSAF regenerative amplifiers or multipass geometrical amplifiers can be seriously considered for a femtosecond laser chain that would then benefits from all the advantages of the LED technology.

Funding: Agence Nationale de la Recherche and Direction Générale de l'Armement (ANR-17-ASTR-0021).

References

1. A. Barbet, F. Balembois, A. Paul, J-P. Blanchot, A-L. Viotti, J. Sabater, F. Druon and P. Georges, Opt. Lett. **39**, 9731 (2014).
2. B. Villars, E. Hill and C. Durfee, Opt. Lett. **40**, 3049 (2015).
3. K-Y. Huang, C-K. Su, M-W. Lin, Y-C. Chiu and Y-C. Huang, Opt. Express **24**, 12043 (2016).
4. C-Y. Cho, C-C. Pu, K-W. Su and Y-F. Chen, Opt. Lett. **42**, 2394 (2017).
5. A. Barbet, A. Paul, T. Gallinelli, F. Balembois, J.-P. Blanchot, S. Forget, S. Chénais, F. Druon and P. Georges Optica **3**, 465 (2016).
6. D. de Boer, D. Bruls and H. Jagt, Opt. Express **24**, A1069 (2016).
7. J. Sathian, J. Breeze, B. Richards, N. McN. Alford and M. Oxborrow, Opt. Expr **25**, 13714 (2017).
8. P. Pichon, A. Barbet, P. Legavre, T. Gallinelli, F. Balembois, J.-P. Blanchot, S. Forget, S. Chénais, F. Druon, and P. Georges, Opt. and Laser Tech. **96**, 7 (2017).
9. P. Pichon, A. Barbet, F. Druon, J.-P. Blanchot, F. Balembois, and P. Georges, Opt. Lett. **42**, 4191 (2017).
10. S. Payne, L. Chase, L. Smith, W. Kway and H.Newkirk, J. Appl. Phys. **66**,1051 (1989).
11. U. Demirbas and I. Baali, Opt. Lett. **40**, 4615 (2015).
12. D. Harter, J. Squier and G. Mourou, Opt. Lett. **17**, 1512 (1992).
13. H. Ahmad, J. of Opt. **24**, 39 (1995).
14. L. Kunpeng, Y. Li, S. Yanlong, H. Chao, Z. Feng, C. Hongwei, H. Ke and Y. Aiping, Opt. and Laser Tech. **74**, 1 (2015).
15. S. Payne, L. Chase, L. Smith, W. Kway and H. Newkirk, Opt. Quantum Electron. **22**, S259 (1990).
16. M. Stadler, B.Chai and M. Bass, Appl. Phys. Lett. **58**, 216 (1991).
17. U. Demirbas and D. Alp Emre Acar, JOSA B **33**, 2105 (2016).
18. F. Balembois, F. Druon, f. Falcoz, P. Georges and A. Brun, Opt. Lett. **22**, 387 (1997).
19. F. Balembois, M. Gaignet, F. Louradour, V. Couderc, A. Barthelemy, P. Georges and A. Brun, App. Phy. B **65**, 255 (1997).
20. F. Balembois, F. Falcoz, F. Kerboull, F. Druon, P. Georges and A. Brun, IEEE J. Quantum Electron. **33**, 1614 (1997).
21. D. Findlay and R. Clay, Phys. Lett. **20**, 277 (1966).
22. C-K. Chang, J-Y. Chang and Y-K. Kuo, Proc. SPIE, 4914, (2002)
23. J. Jabczynski, W. Zendzian, Z. Mierczyk and Z. Frukacz, App. Opt. **40**, 6638 (2001).